Journal of Alloys and Compounds 489 (2010) 674–677

Contents lists available at ScienceDirect

Journal of Alloys and Compounds

journal homepage: www.elsevier.com/locate/jallcom

Nanocrystalline $LiMn_2O_4$ thin film cathode material prepared by polymer spray pyrolysis method for Li-ion battery

S.N. Karthick[a], S. Richard Prabhu Gnanakan[b], A. Subramania[b,*], Hee-Je Kim[a]

[a] Department of Electrical Engineering, Pusan National University, Jangjeon-dong, Geumjeong-gu, Busan 609-735, Republic of Korea
[b] Advanced Materials Research Lab, Department of Industrial Chemistry, Alagappa University, Karaikudi, Tamil Nadu 630 003, India

ARTICLE INFO

Article history:
Received 7 April 2009
Received in revised form
22 September 2009
Accepted 23 September 2009
Available online 2 October 2009

Keywords:
Nanostructured materials
Thin film
$LiMn_2O_4$ cathode
Polymer spray pyrolysis

ABSTRACT

Nanocrystalline cubic spinel lithium manganese oxide thin film was prepared by a polymer spray pyrolysis method using lithium acetate and manganese acetate precursor solution and polyethylene glycol-4000 as a polymeric binder. The substrate temperature was selected from the thermogravimetric analysis by finding the complete crystallization temperature of $LiMn_2O_4$ precursor sample. The deposited $LiMn_2O_4$ thin films were annealed at 450, 500 and 600 °C for 30 min. The thin film annealed at 600 °C was found to be the sufficient temperature to form high phase pure nanocrystalline $LiMn_2O_4$ thin film. The formation of cubic spinel thin film was confirmed by X-ray diffraction study. Scanning electron microscopy and atomic force microscopy analysis revealed that the thin film annealed at 600 °C was found to be nanocrystalline in nature and the surface of the films were uniform without any crack. The electrochemical charge/discharge studies of the prepared $LiMn_2O_4$ film was found to be better compared to the conventional spray pyrolysed thin film material.

1. Introduction

The increasing applications of microlevel thin film battery in various fields such as microsensors, micromechanics, microelectronics, etc., stimulate the research for the development of high performance microlevel secondary batteries like lithium-ion battery. So thin film lithium-ion cells have been regarded as one of the next generation power sources for future ubiquitous environments. Thin film battery is known for their excellent electrochemical properties such as high discharge capacity and higher life cycle. The battery property depends upon three important factors such as nature of cathode, anode and the types of electrolyte used. Various kinds of lithium transition metal oxides have been used as cathode materials for rechargeable lithium batteries [1–4]. Among them, lithium manganese oxide ($LiMn_2O_4$) based materials are of considerable interest as a cathode material because of its less toxicity, low cost, high operating voltage [5,6], etc. But the electrochemical behaviour of $LiMn_2O_4$ cathode depends upon the method of its synthesis. In bulk form [7–9], the electrode is generally prepared by mixing the active oxide with both polymeric binder and high surface area conducting carbon. Because of the effect of high surface area carbon, the material promotes the oxidation of solvent at high potential of operation of the cathode material, leading to irreversible capacity losses [10]. To overcome these disadvantages, thin film electrodes are used to fabricate the battery without using polymeric binder and carbon, so that the electronic contact between active material and current collector was better than powder based electrode material [11–13]. High cost and comparatively tedious thin film methods like electron beam evaporation, RF magnetron, laser ablation, electrostatic spray pyrolysis, chemical vapour deposition, etc. [14–18] have been adapted to synthesis $LiMn_2O_4$ thin filmmaterial.

In the present investigation, a simple, low cost, polymer spray pyrolysis method is used to prepare nanocrystalline $LiMn_2O_4$ thin films. This polymer spray pyrolysis technique required less hardware, simple inexpensive reagents and less sensitive when compared to other thin film techniques. Here the polymer (PEG) plays a vital role to produce nanosize homogeneous particles by enhancing the homogeneous mixing of metal cations, due to its electronegative ether oxygens in the long chain [19,20]. It can easily attract the electropositive metal ions (Li^+ and Mn^{2+}). These Li^+ and Mn^{2+} metal ions are trapped through out the polymer and effectively control the particle size to get the nanocrystalline $LiMn_2O_4$ thin film and also keep the nanosize particles free from agglomeration during the heating process. In normal spray pyrolysis, one can get thin film with submicron size particles. But in the polymer spray pyrolysis process, using polyethylene glycol (PEG) as the polymeric additive, one can get thin film with nanocrystalline particles.

* Corresponding author. Tel.: +91 4565 228836; fax: +91 4565 225202.
E-mail address: a_subramania@yahoo.co.in (A. Subramania).

0925-8388/$ – see front matter © 2009 Elsevier B.V. All rights reserved.
doi:10.1016/j.jallcom.2009.09.147

2. Experimental

2.1. Deposition of $LiMn_2O_4$ thin film

Nanocrystalline $LiMn_2O_4$ thin film cathode material was prepared by a polymer spray pyrolysis method using PEG as the complexing agent. A vertical type spray pyrolysis setup has been used for the experiment. The nozzle size of the spray gun was 0.3 mm. Precursor solution was prepared by dissolving stoichiometric amount of lithium acetate and manganese acetate in water at 1:2 ratio. The molar ratio of PEG to total metal ion concentration was 1:2 ratio. PEG was used as a combustion fuel as well as a polymeric complexing agent for binding Li^+ and Mn^{2+} cations. The long chain polymer is highly dispersive and makes the material most reactive and also act as a metal wrapper as well as a combustion fuel to get nanocrystalline thin film cathode material with good adherence. The stainless steel substrate was cleaned with acetone before use. Pressurized precursor solution at 200 kPa was sprayed on the substrate (kept at 420 °C) through spray nozzle for 20 s. After a time lapse of 240 s, the solution was once again sprayed for 20 s. This was repeated 5–10 times. The substrate temperature was determined from the thermal behaviour of the solution which was followed by thermogravimetric analysis (TGA) using thermal analyzer (PerkinElmer – Diamond) in dynamic air atmosphere at a heating rate of 10 °C/min. The films were calcined for 30 min at 450, 500 and 600 °C to improve the crystallinity of the films.

2.2. Characterization of the films

X-ray diffraction (XRD) measurements were made by JEOL (Model: JDX 8030) X-ray diffractometer using nickel filtered Cu-Kα radiation to identify the phase formation and structural conformation of the deposited $LiMn_2O_4$ thin film cathode material. The diffraction patterns were taken at 25 °C in the range of $0^\circ \leq 2\theta \leq 70^\circ$ in step scans. The step size and scan rate were set at 0.1° and 2°/min, respectively.

The deposited $LiMn_2O_4$ thin film was analysed by Philips (Model: XL30)-scanning electron microscope (SEM) to examine the surface morphology and particle size of the prepared thin film. The surface roughness and particle size of the thin film were investigated by atomic force microscopy (AFM). This topographic surface image was taken using a Nanoscope E – scanning profile microscopy (Model: 3138J).

Finally, the prepared $LiMn_2O_4$ thin film electrode material was subjected to fabricate Li-thin film battery using PVdF-HFP based microporous polymer membrane containing 1 M of $LiPF_6$ in EC:DEC (1:1, v/v) and then the electrochemical charge/discharge studies were performed over the potential range of 3.0–4.5 V at the current density of 0.2 mA/cm^2.

3. Results and discussion

3.1. Thermal studies of $LiMn_2O_4$ precursor sample

Fig. 1 shows the result of thermal analysis on the polymer-salt precursor. It indicates that a continuous weight loss was observed from 70 to 430 °C. It revealed that the solvent evaporation and decomposition of the intermediate complexes of the precursor sample was completed below 430 °C. There was no thermal event beyond 430 °C. Hence, it attributes that the complete crystallization/phase formation temperature of the $LiMn_2O_4$ active material is around 430 °C. This observation was used to fix the substrate temperature for spraying the precursor solution on the substrate at 430 °C for the preparation of $LiMn_2O_4$ thin film.

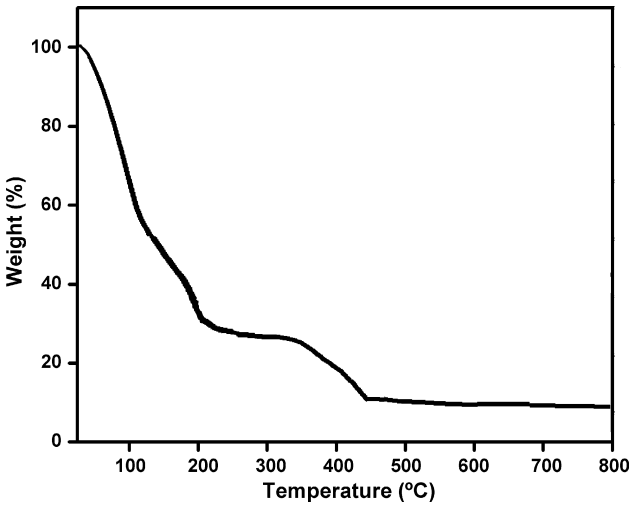

Fig. 1. TGA curve of polymeric precursor sample at the heating rate of 10 °C/min.

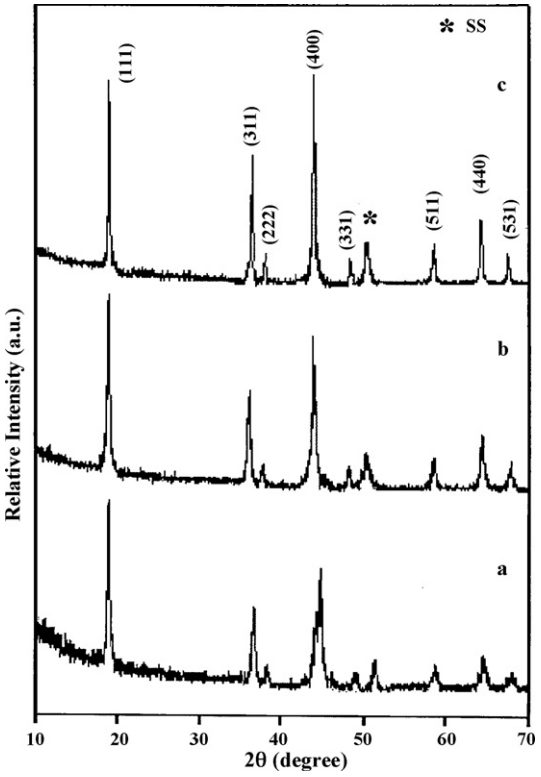

Fig. 2. XRD patterns of $LiMn_2O_4$ thin film annealed at (a) 450 °C, (b) 500 °C, (c) 600 °C for 30 min in air.

3.2. X-ray diffraction studies

X-ray diffraction patterns of the thin film of $LiMn_2O_4$ annealed at 450, 500, 600 °C for 30 min are given in Fig. 2. The diffraction peaks of all the samples were identified as a single phase of cubic spinel structure with the space group *Fd*3*m*. This suggests that annealing does not alter the crystal structure. There was no notable variation of secondary phase or impurities for all the samples. But the intensity of the XRD peaks increased with increase in calcination temperature indicating the enhanced crystallinity of $LiMn_2O_4$ thin film. With further annealing at 700 °C for 30 min, there was no difference in the observed peaks, compared to 600 °C. It shows that the optimum calcination temperature for the formation of well defined crystalline $LiMn_2O_4$ thin film is 600 °C. XRD data were then interpreted with JCPDS (35-0782) data and crystal structure of the $LiMn_2O_4$ thin film was found to be a normal spinel. The well known Debye–Scherer formula was used to calculate the average crystal size [21],

$$L = \frac{0.9\lambda}{\beta \cos\theta} \quad (1)$$

where, λ is the wavelength of X-ray radiation used (in Å), θ the Bragg's angle (in degrees) and β is the full width at half maxima (FWHM in radians). The crystal size and the lattice parameters of all the samples are given in Table 1. The lattice parameter was gradually increased when the annealing temperature increases. The peak (4 0 0) overlapped with that of the substrate peak which cannot be distinguished. The peaks corresponding to the substrate are marked with an asterisk. High intense (1 1 1), (3 1 1) peaks and low intense

Table 1
Lattice parameters and crystal size of $LiMn_2O_4$ thin films in different temperature.

Sample	Temperature (°C)	Crystal size (nm) calculated from Scherer formula	Lattice parameter (Å)	Unit cell volume (Å^3)
$LiMn_2O_4$	450	37	8.1985	551.06
	500	41	8.2252	556.47
	600	45	8.2295	557.38

(3 3 1), (5 1 1) peaks were observed, are the characteristics of cubic spinel structure of $LiMn_2O_4$.

3.3. Morphological properties

The SEM photograph of $LiMn_2O_4$ thin film annealed at 600 °C is shown in Fig. 3a. The surface of the stainless steel substrate was covered with fine crystals. In the entire surface of the thin film peeling off was not observed. The average particles size of the prepared thin film was ~90.7 nm. Compared to normal spray pyrolysis, this method has very small particle size [22]. The nanosized $LiMn_2O_4$ facilitated the rapid diffusion of Li^+ ions, which led to high ionic current and specific capacity [23,24]. Wu et al. [24] have reported the initial capacity for nanosized $LiMn_2O_4$ higher than the corresponding large size materials. The thickness of the $LiMn_2O_4$ thin film was around 0.7 μm as estimated from the cross-section morphology of the thin film (Fig. 3b).

The two dimensional atomic force microscopy (AFM) images showing the surface topography of the deposited $LiMn_2O_4$ thin film on stainless steel substrate at 600 °C are illustrated in Fig. 4a. It showed the fairly rounded particles arrangement. Fig. 4b displays the lateral force microscopic (LFM) images of the corresponding AFM image. The image clearly showed the particles boundary and fairly homogeneous particles arrangement. The film consisted mainly of nanoparticles with an average particles size of 90 nm. The surface of the thin film was densely packed and its root mean square roughness was 24.7 nm.

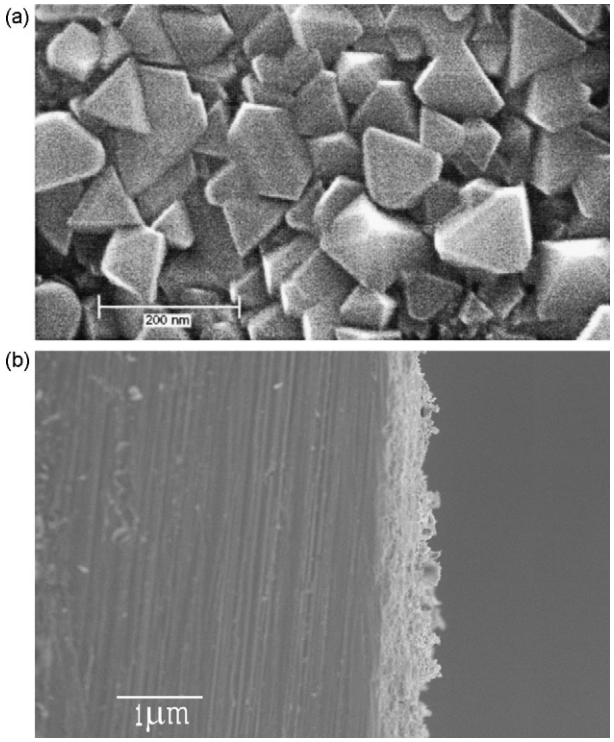

Fig. 3. SEM micrographs of nanocrystalline $LiMn_2O_4$ thin film annealed at 600 °C: (a) surface view and (b) cross-section view.

3.4. Electrochemical properties

Fig. 5 showed the electrochemical behaviour of rechargeable Li//$LiMn_2O_4$ thin film battery at room temperature. The thin film cell was cycled between 3.0 and 4.5 V at a constant current density of 0.2 mA cm^{-2}. It can be seen that two distinct plateaus appear in both the charge and discharge curves. These two step flat plateaus based on the two different lithium ions insertion/extraction processes. While charging, the first and second potential plateaus were at 3.95 and 4.10 V, respectively and during discharge, the potential were located at 4.09 and 3.90 V. It showed that the initial discharge capacity of the thin film $LiMn_2O_4$ was 138 mAh g^{-1} against the theoretical value of 148 mAh g^{-1}. The discharge capacity of the cell decreased slowly to 87.6% of its initial capacity in the 25th cycle. The capacity fading of the thin film prepared in the present study and by the conventional spray pyrolysis method is shown in Fig. 6 for comparison. The figure indicates that a lower capacity fading of 12.4%

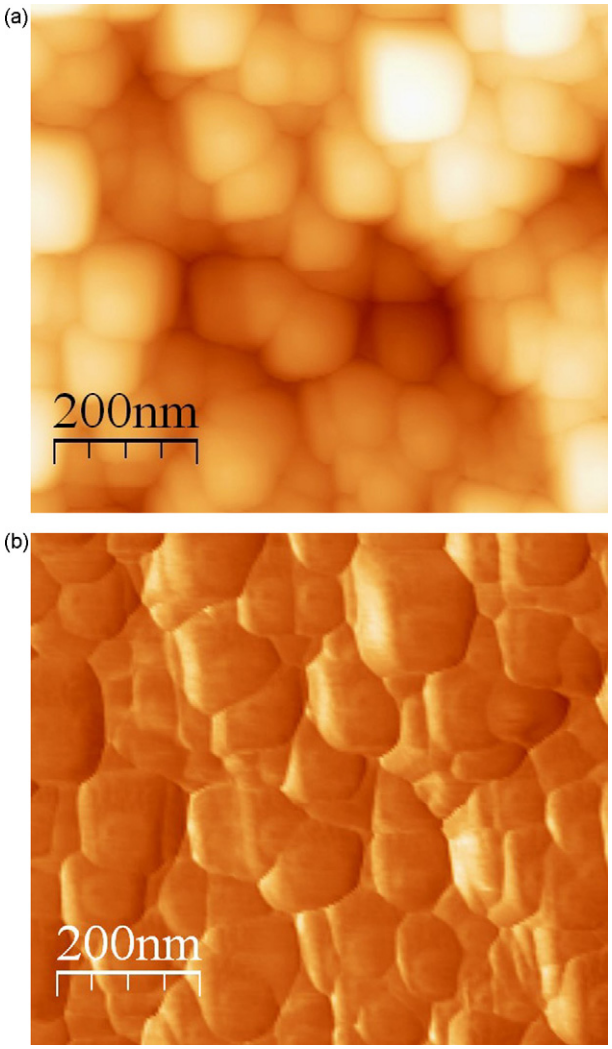

Fig. 4. (a) AFM and (b) LFM topography images of nanocrystalline $LiMn_2O_4$ thin film annealed at 600 °C.

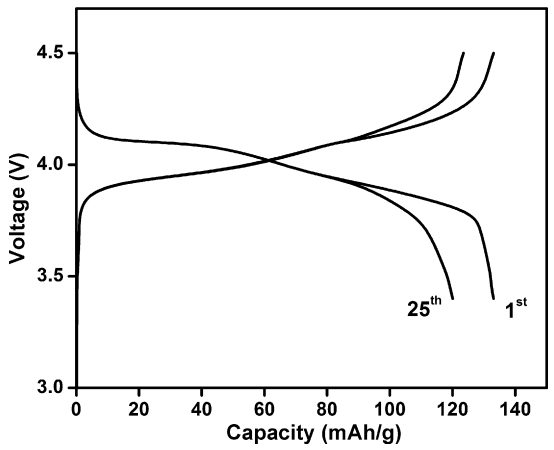

Fig. 5. Charge/discharge plots of Li//$LiMn_2O_4$ thin film cell.

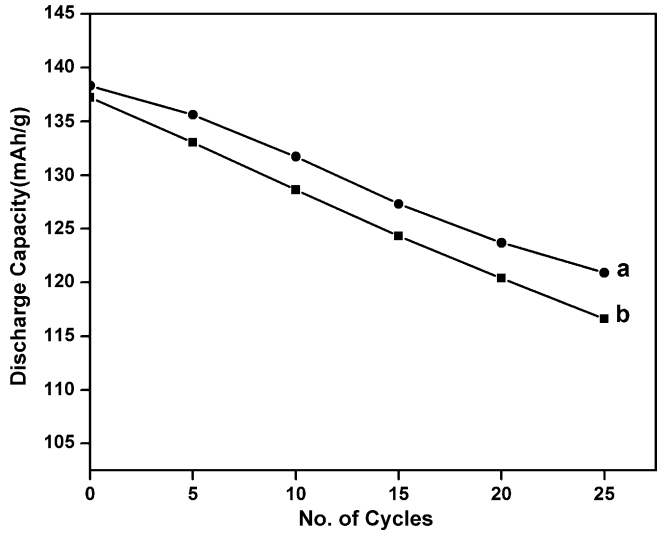

Fig. 6. Relationship between the discharge capacity and cycle number of (a) Li//$LiMn_2O_4$ thin film cell (polymer spray pyrolysis) and (b) Li//$LiMn_2O_4$ thin film cell (conventional spray pyrolysis).

was observed for the polymer spray pyrolysed material, whereas 15% capacity fading was observed for the conventional spray pyrolysed material at 25th cycle [22]. It revealed that the effect of PEG on the preparation of nanocrystalline $LiMn_2O_4$ thin film showed better performance for Li-ion battery. Moreover, the method is inexpensive for the preparation of thin film active materials.

4. Conclusions

The following conclusions are drawn from the above studies:

- Nanocrystalline cubic spinel $LiMn_2O_4$ thin film could be prepared by polymer spray pyrolysis method using PEG as the complexing agent.
- Because of the good gelling and complexing property of PEG, a good adhesion thin film was deposited onto the substrate with no cracks.
- The surface morphology was greatly influenced by the addition of PEG.
- The polymer spray pyrolysed thin film $LiMn_2O_4$ material showed better electrochemical properties such as good capacity and reversibility than the same prepared by the conventional spray pyrolysis method.

References

[1] S.B. Tang, M.O. Lai, L. Lu, J. Alloys Compd. 449 (2008) 300.
[2] C.S. Nimisha, M. Ganapathi, N. Munichandraiah, G. Mohan Rao, Vacuum 83 (2009) 1001.
[3] A. Subramania, N. Angayarkanni, S.N. Karthick, T. Vasudevan, Mater. Lett. 60 (2006) 3023.
[4] C.-J. Kim, I.-S. Ahn, K.-K. Cho, S.-G. Lee, J.-K. Chung, J. Alloys Compd. 449 (2008) 335.
[5] X. Li, Y. Xu, C. Wang, J. Alloys Compd. 479 (2009) 310.
[6] Y. Li, R. Zhang, J. Liu, C. Yang, J. Power Sources 189 (2009) 685.
[7] Q. Liu, L. Yu, H. Wang, J. Alloys Compd. (2009), doi:10.1016/j.jallcom.2009.07.087.
[8] T.J. Patey, R. Buchel, S.H. Ng, F. Krumeich, S.E. Pratsinis, P. Novak, J. Power Sources 189 (2009) 149.
[9] H.-J. Guo, X.-H. Li, Z.-X. Wang, W.-J. Peng, X. Cao, H.-F. Li, J. Power Sources 189 (2009) 95.
[10] D. Guyomard, J.M. Tarascon, J. Electrochem. Soc. 140 (1993) 3071.
[11] A.K. Hjelm, G. Lindbergh, Electrochim. Acta 47 (2002) 1747.
[12] S.B. Tang, H. Xia, M.O. Lai, L. Lu, J. Alloys Compd. 449 (2008) 322.
[13] A. Patil, V. Patil, D.W. Shin, J.-W. Choi, D.-S. Paik, S.-J. Yoon, Mater. Res. Bull. 43 (2008) 1913.
[14] S.B. Tang, M.O. Lai, L. Lu, Electrochim. Acta 52 (2006) 1161.
[15] H.S. Moon, J.W. Park, J. Power Sources 119 (2003) 717.
[16] T. Tsuji, Y. Tatsuyama, M. Tsuji, K. Ishida, S. Okada, J. Yamaki, Mater. Lett. 61 (2007) 2062.
[17] S. Koike, K. Tatsumi, J. Power Sources 146 (2005) 241.
[18] H.-S. Moon, S.W. Lee, Y.-K. Lee, J.-W. Park, J. Power Sources 119–121 (2003) 713.
[19] T. Okada, Analyst 118 (1993) 959.
[20] H.B. Park, Y.S. Hong, J.E. Yi, H.J. Kweon, S.J. Kim, Bull. Korean Chem. Soc. 18 (1997) 612.
[21] H.P. Klug, L.E. Alexander, X-ray Diffraction Procedures for Polycrystalline and Amorphous Materials, Wiley, New York, 1954.
[22] A. Subramania, S.N. Karthick, N. Angayarkanni, Thin Solid Films 516 (2008) 8295.
[23] C.-H. Lu, S.-W. Lin, J. Power Sources 97/98 (2001) 458.
[24] H.M. Wu, J.P. Tu, Y.F. Yuan, Y. Li, W.K. Zhang, H. Huang, Physica B 369 (2005) 221.